

CD40-mediated activation of chronic lymphocytic leukemia cells promotes their CD44-dependent adhesion to hyaluronan and restricts CCL21 induced motility

Tamara Girbl¹, Elisabeth Hinterseer¹, Eva Melanie Grössinger¹, Daniela Asslaber¹, Karin Oberascher², Lukas Weiss¹, Cornelia Hauser-Kronberger³, Daniel Neureiter³, Hubert Kerschbaum², David Naor⁴, Ronen Alon⁵, Richard Greil¹ and Tanja Nicole Hartmann^{1,*}

¹Laboratory for Immunological and Molecular Cancer Research, Third Medical Department with Hematology, Medical Oncology, Hemostaseology, Rheumatology and Infectiology, Paracelsus Medical University, Salzburg, Austria; ²Department of Cell Biology, University of Salzburg, Austria; ³Department of Pathology, Paracelsus Medical University, Salzburg, Austria; ⁴Lautenberger Center of Immunology and Cancer Research, Faculty of Medicine, The Hebrew University of Jerusalem, Israel, ⁵Department of Immunology, Weizmann Institute of Science, Rehovot, Israel

running title: Activational regulation of CD44-mediated adhesion in CLL

key words: CLL, CD44, hyaluronan, adhesion, microenvironment

*Correspondence to: Tanja Nicole Hartmann, Laboratory for Immunological and Molecular Cancer Research, Third Medical Department with Hematology, Medical Oncology, Hemostaseology, Rheumatology and Infectiology, Paracelsus Medical University, Müllner Hauptstrasse 48, 5020 Salzburg, Austria

Tel: +43-662-4482-1552

Fax: +43-662-4482-1570

Email: t.hartmann@salk.at

Abstract

Microenvironmental interactions are crucial for the survival and proliferation of chronic lymphocytic leukemia (CLL) cells. CD4⁺ T cells that express CD40 ligand (CD40L), along with other accessory immune and stromal cells within CLL lymph nodes (LNs) provide signals needed for activation and outgrowth of the tumor clone. Further, correct positioning of CLL cells within lymphoid subcompartments is essential for the transmission of these supportive signals. Thereby, interstitial cell migration and adhesion events, influenced by activational stimuli, determine CLL cell localization. CD44 has been implicated in cell activation, migration and tissue retention via binding to its extracellular matrix ligand hyaluronan (HA). In this study, we investigated the role of CD44-HA interactions for CLL positioning and interaction with supportive microenvironments in peripheral LNs, focusing on its regulation via CD40L-dependent, T cell-mediated activation of CLL cells. We found that HA triggered a robust CCL21-induced motility of resting CLL cells. However, CD40L-stimulation promoted the firm, CD44-mediated adhesion of CLL cells to HA, antagonizing their motile behavior. N-linked glycosylations of CD44, particularly associated with the variant isoform CD44v6 after CD40L-activation, appeared to facilitate HA recognition by CD44. We propose that the CD40L-CD40 signaling axis provides a stop signal to motile CLL cells within LN compartments by inducing high avidity CD44-HA adhesion. This might retain CLL cells close to T cell stimuli and facilitate essential interactions with HA bearing stromal cells, collectively promoting CLL cell proliferation and survival.

Introduction

Chronic lymphocytic leukemia (CLL) is an incurable malignancy of mature B lymphocytes, which progressively accumulate in the peripheral blood (PB), bone marrow (BM) and lymph nodes (LNs). The interaction of CLL cells with accessory cells, the extracellular matrix and soluble factors within the lymphoid microenvironment is essential for CLL cell proliferation and survival (1). CLL cells within lymphoid compartments display an activated CD69⁺ phenotype (2), and their proliferation occurs adjacent to CD40 ligand (CD40L) expressing CD4⁺ T cells and stromal cells within so-called proliferation centers (3, 4). This and further evidence (5, 6), led to the widely accepted concept, that CD4⁺ T lymphocytes play an essential role in CLL cell activation, proliferation and survival. CD40L, a TNF-alpha superfamily member expressed on activated T cells, has been described as key mediator of T cell-driven CLL responses, acting in concert with T cell derived cytokines (7-10).

Healthy T cell-dependent immune responses require the dynamically regulated positioning of B cells to specialized lymphoid subcompartments, which facilitate B cell activation, proliferation and differentiation (11). Activating stimuli alter the responsiveness of chemokine and adhesion receptors and thereby determine B cell migration and retention. LN chemokines co-immobilized to extracellular matrix molecules serve as the respective directional cues (12, 13).

In CLL, little is known about the stop and go signals involved in malignant B cell positioning within the infiltrated LNs, displaying a completely disrupted architecture. CD44 interactions with the extracellular matrix glucosaminoglycan hyaluronan (HA) participate in lymphocyte activation, migration and tissue retention. The CD44 family (panCD44) comprises diverse isoforms, resulting from alternative splicing of 9 variant exons and extensive posttranslational glycosylations and glucosaminoglycan additions. Concomitantly, the HA binding ability of the CD44 molecule is strictly controlled in a cell-type specific manner by CD44 clustering, CD44 variant isoform (CD44v) (14) or glycoform expression (15, 16). In particular,

leukocytes mainly express the standard CD44 isoform (CD44s), which lacks all variant exons, and require stimulation to recognize HA.

Correlative studies have suggested CD44 as a negative prognostic marker in CLL (17-19) but the underlying molecular mechanisms are not fully understood. Here, we aimed to examine the role of CD44-HA interactions for CLL cell positioning within LN compartments. We observed an activation-induced, CD44-mediated adhesion to HA, which was accompanied by increased expression of CD44v6 displaying N-linked glycosylations. We propose that the CD40L-dependent CLL cell activation within LNs may provide a stop signal to motile CLL cells by inducing high avidity CD44-HA interactions, thus contributing to their retention required for survival and proliferation.

Methods

Patient samples. Following informed consent, blood samples were obtained from CLL patients, which were chemo-naïve or had not received chemotherapy during the last 6 months, at the Third Medical Department Salzburg. Peripheral blood mononuclear cells (PBMCs) were obtained by density gradient centrifugation, viably frozen and stored in liquid nitrogen. Thawed PBMCs were cultured in RPMI 1640 medium supplemented with 10% fetal calf serum (FCS) and antibiotics. For functional assays CLL cells were enriched untouched using the EasySep Kit (Stem Cell Technologies). For RNA and protein isolation CLL cells were positively isolated via CD19 microbeads (MACS, Miltenyi). Primary mesenchymal stromal cell cultures were established from BM aspirates from healthy donors as described (20).

CLL cell activation. PBMCs from CLL patients were cultured at a concentration of 2×10^6 /ml for 15 hours on confluent layers of NIH/3T3 murine fibroblasts transfected with human CD40L or empty vectors (MOCK), kindly provided by Katja Zirlik, Freiburg, Germany. NIH/3T3 cells were periodically authenticated by morphological inspection. CD40L expression on CD40L-transfected and control cells was constantly monitored by flow cytometry. For activation by autologous T cells 2×10^6 PBMCs/ml were cultured on MOCK transfected fibroblasts in the presence of human T cell activator CD3/CD28 dynabeads (Invitrogen) for 72 hours. Cells cultured without dynabeads served as unstimulated controls.

Cell lines. Jurkat cells were obtained from the American Type Culture Collection (ATCC), where authentication was performed by DNA fingerprinting with short tandem repeat profiling. After purchase, Jurkat cells were passaged fewer than 6 months. Lysates from HT29, HeLa, HepG2 and A431 cells, which were authenticated by ATCC by short tandem repeat profiling, were purchased from Abcam. MCF-7 cells were kindly provided by Nadia Dandachi (Medical University Graz), passaged fewer than 3 months and used without further authentication.

Antibodies and Reagents. Fluorochrome-labeled monoclonal antibodies (mAbs) were purchased from BD or Beckmann Coulter. Anti-CD44v3 (clone VFF-327v3), anti-CD44v6 (clone VFF-18) and anti-panCD44 mAbs (clone SFF-304) were obtained from eBioscience. The blocking anti-CCR7 mAb (clone 150503) was purchased from R&D and both blocking anti-CD44 mAbs (clone IM7 and 515) from BD. Human or rooster HA, porcine chondroitin sulfate B (CS), hyaluronidase (HAase) from *Streptomyces hyalurolyticus*, recombinant PNGase F and recombinant Endoglycosidases F1 and F2 from *Elizabethkingia miricola* were obtained from Sigma-Aldrich. Fluorescein conjugated HA (FL-HA) was kindly provided by Pauline Johnson, Vancouver, Canada.

Immunofluorescence. Immunofluorescence stains were performed on formaline-fixed, paraffin-embedded LN tissue samples of CLL patients using polyclonal anti-CCL21 (R&D), HA-binding protein (biotinylated, Merck), anti-CD19 (AbD Serotec), anti-Ki-67 (eBioscience) and respective secondary antibodies. Samples were mounted in Prolong Gold antifade reagent with 4',6-diamidino-2-phenylindole (DAPI) (Invitrogen).

Cell motility. Microscopy chambers (Ibidi) were coated with 1 mg/ml HA or CS, followed by 4 µg/ml CCL21 and blocked with 2% human serum albumin (HSA). HA was digested by 30 Units/ml HAase for 1 hour at 37°C. For inhibition experiments, CLL cells were incubated with anti-CCR7 or anti-CD44 mAbs (10 µg/ml) or HA (100 µg/ml) for 15 minutes. 5 minutes after cells were applied to motility chambers, non-interacting cells were washed away. The chambers were placed on a heated (37°C) stage of an inverted phase-contrast microscope (Olympus IX81) and at least 60 cells per field were recorded by time-lapse videomicroscopy using a 20-fold magnification. Cells moving more than 5 cell diameters during the observation time of 1 hour were considered motile. Motile cells and their velocities were determined by manual tracking of single cells using the “Chemotaxis and Migration” plugin of the ImageJ software.

Scanning electron microscopy. 15 minutes after being subjected to HA or HA/CCL21 substrates, CLL cells were fixed with 2.5% glutaraldehyde and dehydrated by ethanol and hexamethyldisilazane. Cells were glued on pins and sputter coated with a 61.2 nm gold layer, before the cell morphology was investigated with a Stereoscan 250 scanning electron microscope (Cambridge Instruments).

Flow cytometry. PBMCs were stained with mAbs specific for CD69, CD80, CD86, CCR7, panCD44, CD44v3, CD44v6 or corresponding isotype controls. To detect soluble HA binding PBMCs were incubated with FL-HA for 15 minutes at 4°C. CD44 was blocked by preincubation with 10 µg/ml anti-CD44 mAb (clone 515). N-linked glycosylations were removed by preincubation with Endoglycosidase F1 and F2 solved in PBS and 2% FCS, according to the manufacturers guidelines. CLL cells were identified by anti-CD5 and anti-CD19 stainings. Viable cells were identified as Annexin V and 7-aminoactinomycin (7-AAD) negative cells.

Adhesion assays. Cell culture-treated dishes were coated with HA (1 mg/ml) overnight, blocked with 2% HSA and assembled as the lower wall of a parallel plate flow chamber (Glycotech). CLL cells were allowed to interact with the substrate for 1 minute before a shear force of 2 dynes/cm² was applied. The percentage of cells remaining adherent for at least 20 seconds was evaluated by manual video analysis. Alternatively, PBMCs were applied to confluent layers of mesenchymal stromal cells. Non-adherent cells were washed away after 20 minutes. Adherent CLL cells, expressed as percentage of total viable input cells, were cytometrically determined using flow-count fluorospheres (Beckman Coulter), anti-CD5 and anti-CD19 mAbs and viability staining. HA was digested by preincubation with 30 Units/ml HAase for 1 hour at 37°C. For blocking experiments CLL cells were pretreated with an anti-CD44 mAb (clone 515, 10 µg/ml) or the respective isotype control.

PCR analyses. Quantitative real-time PCR was performed as described (21). For detection of CD44v transcription by reverse transcription PCR, cDNA from CLL cells was amplified by

panCD44 or CD44 variant exon specific primers as previously described (22) and visualized by 1% agarose ethidium bromide gels.

Immunoblotting. Immunoblotting under denaturing and reducing conditions was performed as described (23) using mAbs specific for panCD44 (clone SFF-304), CD44v3 or CD44v6. For deglycosylation whole cell lysates were digested by PNGase F according to the manufacturer's directions.

Statistical analysis. Statistical analysis was performed using GraphPad Prism 5.0. All data were tested for normal distribution by the Kolmogorov-Smirnov test. Normally distributed data were analyzed by paired t test, non-normally distributed by Wilcoxon matched pairs test. Differences were considered statistically significant when $p < 0.05$.

Results

HA and CCL21 are co-localized within the reticular network of CLL LNs and collectively trigger the robust motility of CLL cells

To identify which LN areas could facilitate CLL cell interactions with HA, we evaluated the HA distribution pattern in LN sections of CLL patients. We found that HA was highly abundant throughout the infiltrated LNs, including sites of low proliferation (Figure 1A, left), as well as CLL cell proliferation centers, determined by the accumulation of Ki-67+ CLL cells (Figure 1A, right). CLL cells were determined by CD19/CD5 co-staining (data not shown). This suggests that resting as well as proliferating CLL cells are in close contact with HA.

To better understand the physiological role of HA for CLL cells within LNs, we established an *in vitro* system to determine the lateral migration of CLL cells on immobilized HA in the presence or absence of co-immobilized chemokines by time-lapse videomicroscopy. We observed that HA on its own failed to support the spontaneous migration of unactivated CLL cells. In contrast, surfaces displaying HA co-immobilized with CCL21 (herein HA/CCL21)

induced CLL cells to migrate randomly with an average velocity of $5.0 \pm 1.6 \mu\text{m}/\text{min}$ (Figure 1B). CCL19 and CXCL13, two other chemokines contributing to B cell positioning within the LNs, induced a less robust migratory response (data not shown), wherefore we focused our studies on CCL21.

Scanning electron microscopy illustrated the round morphology of CLL cells positioned on HA, reflecting their non-motile phenotype. However, CLL cells on HA/CCL21 gained a polarized morphology with highly branched membrane projections and large lamellipodia, indicating cell locomotion (Figure 1C).

The CCL21-induced movement on HA was dependent on the chemokine receptor CCR7, as demonstrated by blocking experiments (Figure 1D). Additionally, the presence of high molecular weight HA was indispensable, since the enzymatic treatment of HA/CCL21 coatings with HAase diminished cell motility. Consistently, CCL21 co-immobilized with CS, another glucosaminoglycan chemically closely related to HA, failed to support CLL cell locomotion (Figure 1E). CD44 blockage with the mAb clone IM7 did not affect the cell motility (Figure 1F), while blockage using a different clone (515) even enhanced the motile response (data not shown), suggesting that HA-mediated motility in CLL was triggered by a CD44 independent pathway(s). This is in line with previous observations describing HA/IL-8-induced motility of CLL cells being mediated by the receptor for hyaluronan-mediated motility (RHAMM) (24).

To verify that CLL cells simultaneously encounter HA and CCL21 *in vivo*, we next assessed their relative distribution by fluorescence co-stainings. CCL21 was distributed throughout the infiltrated LNs, and co-localized with HA at the reticular network, previously suggested to serve as guiding structure for leukocyte migration (Figure 1G) (25).

CD40L-stimulation of CLL cells induces an activated phenotype with reduced motility on immobilized HA/CCL21

Next, we determined how CD40L stimulation, supposed to occur in LNs, influences the CLL cell phenotype and migratory behavior on HA/CCL21. To mimic T cell support, we stimulated PB derived CLL cells *in vitro* by CD40L-transfected fibroblasts, or activated autologous T cells.

CLL cells cultured on CD40L-overexpressing fibroblasts gained an activated phenotype with strongly increased CD69, CD80 and CD86 surface levels as compared to cells cultured on control fibroblasts (Figure 2A). Co-culture with activated, autologous T cells induced a comparable activated CLL cell phenotype (Figure 2B) followed by their proliferation (Supplementary Figure S1).

Because the fibroblast based CD40L activation system generated highly homogeneous activation profiles among all patient samples, we performed functional studies with this system, but confirmed key findings on CLL cells stimulated with activated T cells.

By time-lapse videomicroscopy we investigated how activation modulates the migratory behavior of CLL cells on HA/CCL21. The motility of CD40L-stimulated cells was significantly decreased compared to unstimulated controls (Figure 2C). CD40L-activated CLL cells expressed higher CCR7 levels than unstimulated controls (Figure 2D) and fully retained their chemotactic response towards soluble CCL21 in transwell assays (Supplementary Figure S2). Thus, the reduced migration of CD40L-activated CLL cells on HA/CCL21 coatings did not result from a decreased CCL21 responsiveness, but rather from their altered interaction with HA. This prompted us to investigate a potential difference of HA binding properties in unstimulated and CD40L-activated CLL cells.

CD40L-activation induces a strong HA binding in CLL cells, which is entirely CD44-mediated

Cell migration requires an intermediate attachment strength between a cell and its substrate, enabling the generation of traction force to pull the cell forward but also permitting retraction

of the cell rear (26). Therefore, we tested the binding of CLL cells to soluble FL-HA via flow cytometry. Although unstimulated CLL cells interacted with immobilized HA through weak interactions, which promoted their motility, these cells failed to bind soluble FL-HA, reflecting a rather weak affinity for HA. In contrast, FL-HA binding was observed in a considerable portion of CD40L-activated CLL cells and was entirely CD44-mediated as shown by blocking experiments (Figure 3A). Similarly, CLL cells co-cultured with activated T cells showed comparable levels of HA-binding (Figure 3B). Notably, this binding was also inducible by other stimuli, e.g. PMA/ionomycin or IgM-crosslinking (Supplementary Figure S3), suggesting that HA-binding is a general phenomenon of CLL cell activation rather than an exclusive effect of CD40L-stimulation.

To confirm that the CD44-HA bonds triggered by CD40L-activation are sufficient to mediate CLL cell adhesion, we next measured the ability of CLL cells to adhere to immobilized HA and withstand a sudden shear force. While the majority of unstimulated CLL cells failed to develop shear resistant adhesions, CD40L-stimulation induced a strong CD44-mediated HA-dependent shear resistant adhesion (Figure 3C), which was not affected by the presence of CCL21 (data not shown). Furthermore, the ability of CD40L to stimulate CD44 adhesiveness to HA appeared specialized, because CLL adhesion to other ECM ligands like fibronectin, collagen type I, and laminin remained negligible (data not shown).

CD40L-induced CD44-HA bonds “lock” CLL cells to HA and overrule CCL21-mediated promigratory signals

To confirm that the high avidity CD44-HA interactions by themselves are responsible for the reduced motility of CD40L activated CLL cells on HA/CCL21, we blocked these interactions by preincubation with saturating amounts of soluble HA (sHA). Indeed, this restored the motile phenotype of CD40L-stimulated CLL cells on the HA/CCL21 substrate (Figure 4A). SHA treatment also reduced the adhesion of CD40L-activated CLL cells to immobilized HA

confirming its blocking effect on CD44-HA bonds (Figure 4B, left). Instead, cell rolling under shear force was increased (Figure 4B, right), pointing to HA-dependent interactions of a lower strength. These results show that CD40L-activation *per se* did not alter the migratory potential of CLL cells on HA/CCL21 but induced strong CD44-mediated adhesions to HA, which locked CLL cells to the substrate and thereby overruled the CCL21-mediated promigratory signal.

CD40L-stimulation elevates panCD44 levels and induces the expression of the variant isoforms CD44v3 and CD44v6

The differential capacity of CD44 on unstimulated and CD40L-activated CLL cells to bind HA led us to investigate potential alterations in their panCD44 levels or structural changes within the expressed CD44 repertoire. We found a transcriptional upregulation of panCD44 upon CD40L-activation (Figure 5A), which translated into a significantly increased surface expression (Figure 5B). However, all CLL patients, irrespective of their clinical risk profile, uniformly displayed high panCD44 levels on PB CLL cells, which poorly bound HA (Supplementary Figure S4). Therefore, the induction of HA binding only by increased panCD44 surface levels is improbable and we investigated CD44v expression of CLL cells.

CD44 encoded, mature mRNA of unstimulated CLL cells contained the variant exons v3, v5, v6, v7, v8, v9 and v10, as detected by reverse transcription PCR. Particularly v3 and v6 were increased upon CD40L stimulation (Figure 5C). Consistently, CD40L-activation increased the surface expression of CD44 isoforms containing v3 and v6 (CD44v3 and CD44v6) (Figure 5D). A small population of CLL cells remained CD44v6 negative and displayed low CD86 expression, indicating a low activation level (Supplementary Figure S5). CD44v6 expression and the HA binding capacity was induced simultaneously in CLL cells cultured on CD40L-expressing fibroblasts (Figure 5E). Confirmingly, CLL cell activation by activated T cells

caused increased panCD44 and CD44v6 surface expression (Figure 5F), whereas CD44v3 remained unaffected (data not shown).

N-linked glycosylations, possibly linked to CD44v6, facilitate HA binding of CD44

To detect if CD40L-triggered alterations in CD44 glycoform expression could facilitate its HA binding capacity, we analyzed the molecular weight of CD44 by immunoblotting with or without removal of N-linked glycosylation by PNGase F. Using the panCD44 mAb, we found basal N-linked glycosylations of the predominant, ~90 kDa CD44 iso/glycoform, which were unaffected by the CLL activation status (Figure 6A). CD40L-stimulation induced the expression of CD44v6, with the high molecular weight of ~150 kDa, which was reduced after PNGase F treatment (Figure 6B). Negative and positive controls proved the specificity of the used mAbs (Supplementary Figure S6).

The removal of N-linked glycans by Endoglycosidase F1 and F2 decreased FL-HA binding of CD40L-activated CLL cells (Figure 6C). This shows that HA binding properties of CD44 on CD40L-activated CLL cells are at least partially facilitated by N-linked glycosylations, found to be associated with CD44v6 but potentially also other isoforms.

CD40L-activation potentiates the adhesion of CLL cells to primary stromal cells in a CD44-dependent manner

Stromal contact within the LN microenvironment is thought to support CLL outgrowth and survival. Therefore, we determined the importance of CD44-mediated adhesions to HA-bearing primary mesenchymal stromal cells. We found that CD40L-stimulation highly increased CLL cell adhesion compared to unstimulated control cells (Figure 7), which was largely CD44-mediated as shown by blocking experiments. An isotype matched control mAb had no effect (data not shown). The adhesion was also HA dependent, as HAase treatment of stromal cells decreased CLL cell adhesion (Figure 7).

Discussion

CLL cells are known to interact with CD40L⁺ T cells within the lymphoid microenvironment thereby receiving survival- and proliferation-inducing signals (4). To date, molecular cues determining CLL cell positioning and retention in proximity to the supportive signals remain poorly defined.

We found that CLL cells that were activated via the CD40-CD40L axis used HA as a substrate for CD44(v)-mediated adhesion. This was accompanied by induction of CD44v isoforms carrying N-linked glycosylations, altering the CD44 affinity to HA. These strong interactions inhibited the HA-dependent motility by locking CLL cells to immobilized HA and overruled CCL21-mediated promigratory signals. We suggest that unstimulated CLL cells utilize the reticular network, simultaneously presenting HA and CCL21, for their interstitial migration. Once CLL cells encounter T cells, they presumably get activated via CD40-CD40L signaling. This induces strong CD44(v)-HA bindings, causing CLL cells to stop migrating and instead tightly adhere to HA-bearing stromal cells. Importantly, HA and Ki-67 stainings of CLL LNs verified strong HA expression at areas of high CLL cell proliferation. We propose that their CD44-HA dependent adhesion facilitates cell division by retaining CLL cells in close proximity to CD4⁺ T cells, providing survival- and proliferation-inducing signals, e.g. T cell-derived interleukines.

Tumor-driving CD44-HA interactions have been described in a variety of cancers (27). In CLL, elevated CD44 serum levels and high panCD44 as well as CD44v surface levels have been suggested as prognostic markers. While apparent consensus exists on the association of high CD44 serum levels with poor clinical outcome (17, 18, 28), the prognostic relevance of panCD44 and CD44v surface levels on circulating CLL cells remains arguable. Our data do not support a prognostic value of high CD44 levels on PB CLL cells. Instead, we suggest CD44v to be increased on CLL cells upon their activation by T cells in lymphoid organs preceding their proliferation. Increased CD44v expression on circulating CLL cells in

patients with poor outcome (19) might thus reflect their activated phenotype. It is reasonable to assume that CD44 is shed from the CLL cell surface by e.g. matrix metalloproteinases (29) after proliferation to disrupt their anchorage on the HA substrate and to restore their interstitial motility. This shedding might account for the increased CD44 serum levels observed in CLL cases with high proliferative activity.

CD44(v)-HA interactions likely contribute to CLL cell survival. Multiple studies have implicated that direct cell contact with stromal cells rescues CLL cells from spontaneous and drug induced apoptosis (30, 31). We observed that CD40L-activation significantly elevated the CD44-HA-mediated adhesion of CLL cells to mesenchymal stromal cells. CD44 signaling has been suggested to activate prosurvival pathways via Mcl-1 (32, 33) or CD44v complexing with VLA-4 and MMP-9, facilitating prosurvival signals via the hemopoxin domain of MMP-9 in CLL (34, 35). However, we did not observe a survival benefit of CD40L activated CLL cells plated on isolated HA (data not shown), suggesting that CD44 *per se* did not induce prosurvival signals upon engagement with HA, but instead established and/or maintained close contact to stromal cells, enhancing the transmission of stromal-derived survival signals. Prognostic potential and microenvironmental relevance have also been attributed to RHAMM, a second HA receptor in CLL (36). RHAMM and CD44 can act as competing molecules or compensate each other regarding HA-mediated functions (37, 38). Previous observations in CLL suggested a clear RHAMM-dependency of IL-8/HA-induced CLL cell motility (24). As CD44 was not accountable for HA/chemokine-induced motility of resting CLL cells but mediated strong HA adhesion of CD40L-activated CLL cells, we suggest a well-regulated balance of RHAMM-HA and CD44-HA interactions in this disease.

Notably, we found that N-linked glycosylations support HA recognition by CD44 on activated CLL cells, in line with previous studies on melanoma cells (15). As CD40L-activation did not affect glycosylations of the basal CD44 iso/glycoform but particularly induced the expression of N-glycosylated CD44v6, we suggest that HA recognition is mediated by variant isoforms

and depends on their glycosylation patterns. While the exact mechanism remains elusive in this study, we assume that N-linked glycosylations trigger HA binding in CLL by altering CD44v charge and/or structure, or more indirectly, by facilitating CD44 clustering, which enables strong HA binding.

Collectively, our study provides strong evidence that microenvironmental interactions of activated CLL cells preceding their proliferation within LNs are facilitated by CD44(v)-HA interactions. Therefore, a disruption of these bonds could represent a promising therapeutic approach. The targeting of distinct CD44 isoforms/glycoforms, having a restricted expression pattern would allow specific targeting of CD44-HA adhesions and circumvent some of the previously observed side-effects raised by potential therapies targeting ubiquitously expressed panCD44 (39). Taken together, we propose that the interference with CD44(v) mediated adhesions to HA could release the tumor cells from their protective niches, prevent their proliferation, and eventually provide strong synergism with conventional therapies.

Acknowledgments

This work has been supported by the Austrian Science Fund FWF (W1213 and SFB P021 to R.G., P25015-B13 to T.N.H.), the Austrian National Bank (13420 to T.N.H., 14311 to R.G., the Paracelsus Medical University Salzburg (E-10/11/058-HAR to T.N.H), the “Klinische Malignom- und Zytokinforschung Salzburg-Innsbruck GmbH”, and the province of Salzburg. The authors thank Karin Stefanon for skillful sample preparation and Josefina Pinon-Hofbauer for helpful discussions.

Authorship

The authors have no conflict of interest to declare.

References

1. Deaglio S, Malavasi F. Chronic lymphocytic leukemia microenvironment: shifting the balance from apoptosis to proliferation. *Haematologica*. 2009;94:752-6.
2. Herishanu Y, Perez-Galan P, Liu D, Biancotto A, Pittaluga S, Vire B, et al. The lymph node microenvironment promotes B-cell receptor signaling, NF-kappaB activation, and tumor proliferation in chronic lymphocytic leukemia. *Blood*. 2011;117:563-74.
3. Granziero L, Ghia P, Circosta P, Gottardi D, Strola G, Geuna M, et al. Survivin is expressed on CD40 stimulation and interfaces proliferation and apoptosis in B-cell chronic lymphocytic leukemia. *Blood*. 2001;97:2777-83.
4. Patten PE, Buggins AG, Richards J, Wotherspoon A, Salisbury J, Mufti GJ, et al. CD38 expression in chronic lymphocytic leukemia is regulated by the tumor microenvironment. *Blood*. 2008;111:5173-81.
5. Bagnara D, Kaufman MS, Calissano C, Marsilio S, Patten PE, Simone R, et al. A novel adoptive transfer model of chronic lymphocytic leukemia suggests a key role for T lymphocytes in the disease. *Blood*. 2011;117:5463-72.
6. Tinhofer I, Weiss L, Gassner F, Rubenzer G, Holler C, Greil R. Difference in the Relative Distribution of CD4+ T-cell Subsets in B-CLL With Mutated and Unmutated Immunoglobulin (Ig) VH Genes: Implication for the Course of Disease. *J Immunother*. 2009.
7. Fluckiger AC, Rossi JF, Bussel A, Bryon P, Banchereau J, Defrance T. Responsiveness of chronic lymphocytic leukemia B cells activated via surface Igs or CD40 to B-cell tropic factors. *Blood*. 1992;80:3173-81.
8. Kitada S, Zapata JM, Andreeff M, Reed JC. Bryostatin and CD40-ligand enhance apoptosis resistance and induce expression of cell survival genes in B-cell chronic lymphocytic leukaemia. *Br J Haematol*. 1999;106:995-1004.
9. Dancescu M, Rubio-Trujillo M, Biron G, Bron D, Delespesse G, Sarfati M. Interleukin 4 protects chronic lymphocytic leukemic B cells from death by apoptosis and upregulates Bcl-2 expression. *J Exp Med*. 1992;176:1319-26.
10. Plander M, Seegers S, Ugocsai P, Diermeier-Daucher S, Ivanyi J, Schmitz G, et al. Different proliferative and survival capacity of CLL-cells in a newly established in vitro model for pseudofollicles. *Leukemia*. 2009;23:2118-28.
11. Pereira JP, Kelly LM, Cyster JG. Finding the right niche: B-cell migration in the early phases of T-dependent antibody responses. *Int Immunol*. 2010;22:413-9.
12. Cyster JG. Chemokines and cell migration in secondary lymphoid organs. *Science*. 1999;286:2098-102.
13. Johrer K, Hofbauer SW, Zelle-Rieser C, Greil R, Hartmann TN. Chemokine-dependent B cell-T cell interactions in chronic lymphocytic leukemia and multiple myeloma - targets for therapeutic intervention? Expert opinion on biological therapy. 2012.
14. Wallach-Dayana SB, Grabovsky V, Moll J, Sleeman J, Herrlich P, Alon R, et al. CD44-dependent lymphoma cell dissemination: a cell surface CD44 variant, rather than standard CD44, supports in vitro lymphoma cell rolling on hyaluronic acid substrate and its in vivo accumulation in the peripheral lymph nodes. *J Cell Sci*. 2001;114:3463-77.
15. Bennett KL, Modrell B, Greenfield B, Bartolazzi A, Stamenkovic I, Peach R, et al. Regulation of CD44 binding to hyaluronan by glycosylation of variably spliced exons. *J Cell Biol*. 1995;131:1623-33.
16. Maiti A, Maki G, Johnson P. TNF-alpha induction of CD44-mediated leukocyte adhesion by sulfation. *Science*. 1998;282:941-3.
17. De Rossi G, Marroni P, Paganuzzi M, Mauro FR, Tenca C, Zarcone D, et al. Increased serum levels of soluble CD44 standard, but not of variant isoforms v5 and v6, in B cell chronic lymphocytic leukemia. *Leukemia*. 1997;11:134-41.

18. Eisterer W, Bechter O, Soderberg O, Nilsson K, Terol M, Greil R, et al. Elevated levels of soluble CD44 are associated with advanced disease and in vitro proliferation of neoplastic lymphocytes in B-cell chronic lymphocytic leukaemia. *Leuk Res.* 2004;28:1043-51.
19. Zarcone D, De Rossi G, Tenca C, Marroni P, Mauro FR, Cerruti GM, et al. Functional and clinical relevance of CD44 variant isoform expression on B-cell chronic lymphocytic leukemia cells. *Haematologica.* 1998;83:1088-98.
20. Jaganathan BG, Ruester B, Dressel L, Stein S, Grez M, Seifried E, et al. Rho inhibition induces migration of mesenchymal stromal cells. *Stem Cells.* 2007;25:1966-74.
21. Desch P, Asslaber D, Kern D, Schnidar H, Mangelberger D, Alinger B, et al. Inhibition of GLI, but not Smoothed, induces apoptosis in chronic lymphocytic leukemia cells. *Oncogene.* 2010;29:4885-95.
22. van Weering DH, Baas PD, Bos JL. A PCR-based method for the analysis of human CD44 splice products. *PCR methods and applications.* 1993;3:100-6.
23. Merkel O, Heyder C, Asslaber D, Hamacher F, Tinhofer I, Holler C, et al. Arsenic trioxide induces apoptosis preferentially in B-CLL cells of patients with unfavourable prognostic factors including del17p13. *J Mol Med.* 2008;86:541-52.
24. Till KJ, Zuzel M, Cawley JC. The role of hyaluronan and interleukin 8 in the migration of chronic lymphocytic leukemia cells within lymphoreticular tissues. *Cancer Res.* 1999;59:4419-26.
25. Bajenoff M, Egen JG, Koo LY, Laugier JP, Brau F, Glaichenhaus N, et al. Stromal cell networks regulate lymphocyte entry, migration, and territoriality in lymph nodes. *Immunity.* 2006;25:989-1001.
26. Li S, Guan JL, Chien S. Biochemistry and biomechanics of cell motility. *Annual review of biomedical engineering.* 2005;7:105-50.
27. Naor D, Nedvetzki S, Golan I, Melnik L, Faitelson Y. CD44 in cancer. *Critical reviews in clinical laboratory sciences.* 2002;39:527-79.
28. Molica S, Vitelli G, Levato D, Giannarelli D, Gandolfo GM. Elevated serum levels of soluble CD44 can identify a subgroup of patients with early B-cell chronic lymphocytic leukemia who are at high risk of disease progression. *Cancer.* 2001;92:713-9.
29. Vagima Y, Avigdor A, Goichberg P, Shivtiel S, Tesio M, Kalinkovich A, et al. MT1-MMP and RECK are involved in human CD34+ progenitor cell retention, egress, and mobilization. *J Clin Invest.* 2009;119:492-503.
30. Burger M, Hartmann T, Krome M, Rawluk J, Tamamura H, Fujii N, et al. Small peptide inhibitors of the CXCR4 chemokine receptor (CD184) antagonize the activation, migration, and antiapoptotic responses of CXCL12 in chronic lymphocytic leukemia B cells. *Blood.* 2005;106:1824-30.
31. Kurtova AV, Balakrishnan K, Chen R, Ding W, Schnabl S, Quiroga MP, et al. Diverse marrow stromal cells protect CLL cells from spontaneous and drug-induced apoptosis: development of a reliable and reproducible system to assess stromal cell adhesion-mediated drug resistance. *Blood.* 2009;114:4441-50.
32. Herishanu Y, Gibellini F, Njuguna N, Hazan-Halevy I, Farooqui M, Bern S, et al. Activation of CD44, a receptor for extracellular matrix components, protects chronic lymphocytic leukemia cells from spontaneous and drug induced apoptosis through MCL-1. *Leuk Lymphoma.* 2011;52:1758-69.
33. Pedersen IM, Kitada S, Leoni LM, Zapata JM, Karras JG, Tsukada N, et al. Protection of CLL B cells by a follicular dendritic cell line is dependent on induction of Mcl-1. *Blood.* 2002;100:1795-801.
34. Redondo-Munoz J, Ugarte-Berzal E, Garcia-Marco JA, del Cerro MH, Van den Steen PE, Opdenakker G, et al. Alpha4beta1 integrin and 190-kDa CD44v constitute a cell surface

docking complex for gelatinase B/MMP-9 in chronic leukemic but not in normal B cells. *Blood*. 2008;112:169-78.

35. Redondo-Munoz J, Ugarte-Berzal E, Terol MJ, Van den Steen PE, Hernandez del Cerro M, Roderfeld M, et al. Matrix metalloproteinase-9 promotes chronic lymphocytic leukemia b cell survival through its hemopexin domain. *Cancer Cell*. 2010;17:160-72.

36. Giannopoulos K, Mertens D, Buhler A, Barth TF, Idler I, Moller P, et al. The candidate immunotherapeutical target, the receptor for hyaluronic acid-mediated motility, is associated with proliferation and shows prognostic value in B-cell chronic lymphocytic leukemia. *Leukemia*. 2009;23:519-27.

37. Nedvetzki S, Gonen E, Assayag N, Reich R, Williams RO, Thurmond RL, et al. RHAMM, a receptor for hyaluronan-mediated motility, compensates for CD44 in inflamed CD44-knockout mice: a different interpretation of redundancy. *Proc Natl Acad Sci U S A*. 2004;101:18081-6.

38. Naor D, Nedvetzki S, Walmsley M, Yayon A, Turley EA, Golan I, et al. CD44 involvement in autoimmune inflammations: the lesson to be learned from CD44-targeting by antibody or from knockout mice. *Ann N Y Acad Sci*. 2007;1110:233-47.

39. Orian-Rousseau V. CD44, a therapeutic target for metastasising tumours. *Eur J Cancer*. 2010;46:1271-7.

Figure Legends

Figure 1: HA and CCL21 are co-localized within the reticular network of CLL LNs and collectively trigger the robust motility of CLL cells. (A) Fluorescence images representative for 3 patients analyzed, show HA (green) and Ki-67 (orange) in combination with nuclear DAPI (white) stains of consecutive CLL LN sections. Scale bars represent 50 μm . (B) CLL cell motility on immobilized HA with or without CCL21 was analyzed by time-lapse videomicroscopy (n=10). (C) Representative scanning electron images show CLL cell morphology on immobilized HA or HA/CCL21. Scale bars represent 5 μm . (D) CLL cells were pretreated with a blocking anti-CCR7 mAb before being subjected to immobilized HA/CCL21 (n=6). (E) Cell motility on HA/CCL21 coatings treated with hyaluronidase (HAase) and untreated coatings (n=2). Where indicated, CLL cell motility on chondroitin sulfate (CS)/CCL21 was compared to HA/CCL21 coatings (n=5). (F) CLL cells were pretreated with a blocking anti-CD44 mAb (n=2). (G) Fluorescence images, representative for 3 patients, show HA and CCL21 co-stainings within the reticular network of a CLL LN section. The scale bar represents 20 μm .

Figure 2: CD40L-stimulation of CLL cells induces an activated phenotype with reduced motility on immobilized HA/CCL21. Cytometrical analysis of CD69, CD80 or CD86 expression on CLL cells co-cultured with (A) MOCK- (w/o CD40L) or CD40L-transfected NIH/3T3 fibroblasts, representative for at least 8 patients measured, or (B) on CLL cells cultured with autologous T cells on fibroblasts in the absence (w/o T_{act}) or presence (+T_{act}) of CD3/CD28 dynabeads. The data are representative for 8 patients analyzed. (C) CLL cell motility on HA/CCL21 after CD40L-stimulation was analyzed as described (n=9). (D) Cytometrical analysis of CCR7 expression on unstimulated and CD40L-activated CLL cells representative for 8 patients. Bars represent the mean \pm SD; **p<0.01.

Figure 3: CD40L-activation induces a strong HA binding in CLL cells, which is entirely CD44-mediated. (A) Cytometrical analysis of soluble FL-HA binding to unstimulated or CD40L-stimulated CLL cells (n=10, left). Where indicated CLL cells were pretreated with a blocking anti-CD44 or isotype-matched control mAb (IgG₁) (n=6, right). Results are illustrated in box plot format, whereby the median, the 25th and 75th percentile and the minimum and maximum observations are depicted. (B) Cytometrical analysis of FL-HA binding of CLL cells after stimulation with activated T cells (n=9). (C) Shear resistant adhesion of unstimulated or CD40L-activated CLL cells on immobilized HA (n=8, left). Where indicated CLL cells were pretreated with a blocking anti-CD44 mAb or isotype control (IgG₁) (n=6, right). *p<0.05; **p<0.01; ***p<0.001.

Figure 4: CD40L-induced CD44-HA bonds “lock” CLL cells to HA and overrule CCL21-mediated promigratory signals. (A) CD40L-stimulated CLL cells were pretreated with sHA to block high avidity interactions with immobilized HA. The motility on HA/CCL21 was determined by videomicroscopy (n=6). (B) CD40L-stimulated CLL cells were left untreated or incubated with sHA prior to the analysis of shear resistant adhesion (left) and rolling (right) on HA-coated plates or control plates lacking HA (n=5). Bars represent the mean ± SD; *p<0.05; **p<0.01.

Figure 5: CD40L-stimulation elevates panCD44 levels and induces the expression of the variant isoforms CD44v3 and CD44v6. (A) Relative panCD44 transcript levels in unstimulated or CD40L-activated CLL cells were determined by real-time PCR (n=6). Data are shown in box-plot format. (B) Representative fluorescence histograms (left) and MFI ratios (right) of panCD44 surface levels on unstimulated or CD40L-activated CLL cells as determined cytometrically (n=11). (C) Reverse transcription PCR analysis of variant exons in the CD44 cDNA from control or CD40L activated CLL cells. The schema illustrates the

CD44 mRNA with the binding regions of the variant exon specific, or panCD44 forward primers (arrows) used in combination with a constant exon specific reverse primer. Double bands indicate the existence of additional variant exons within the amplified region. GAPDH primers were used as loading controls. The inverted agarose gel images depict data from one patient representative for 5 analyzed. (D) Left: Representative fluorescence histograms (left) and MFI ratios (right) of CD44v3 (n=7) and CD44v6 (n= 9) stainings on unstimulated and CD40L-activated CLL cells. (E) PBMCs were cultured on CD40L-expressing fibroblasts for the indicated time points. Kinetics of CD44v3 and CD44v6 expression and its relation to FL-HA binding were determined cytometrically. One of two patients measured is shown. (F) The percentages of pan CD44 or CD44v6 positive CLL cells, cultured with unactivated or activated T cells on fibroblasts. * $p < 0.05$; *** $p < 0.001$.

Figure 6: N-linked glycosylations, possibly linked to CD44v6, facilitate HA binding of CD44. Immunoblotting was performed with unactivated and CD40L-stimulated CLL cells. Where indicated N-linked glycans were removed from whole cell lysates by PNGase F. Bands visualized by anti-panCD44 (A), anti-CD44v6 (B) or anti-CD5 (loading control) mAbs are illustrated by the inverted immunoblot images representative for 3 patients analyzed. (C) N-linked glycosylations were removed by Endoglycosidase F1 and F2 before FL-HA binding to viable CD40L-activated CLL cells was measured cytometrically. * $p < 0.05$.

Figure 7: CD40L-activation potentiates the adhesion of CLL cells to primary stromal cells in a CD44-dependent manner. The adhesion of unstimulated or CD40L activated CLL cells to primary mesenchymal stromal cells. Where indicated cells were pretreated with a blocking anti-CD44 mAb or stromal cells were treated with HAase before CLL cells were applied (n=8). ** $p < 0.01$.

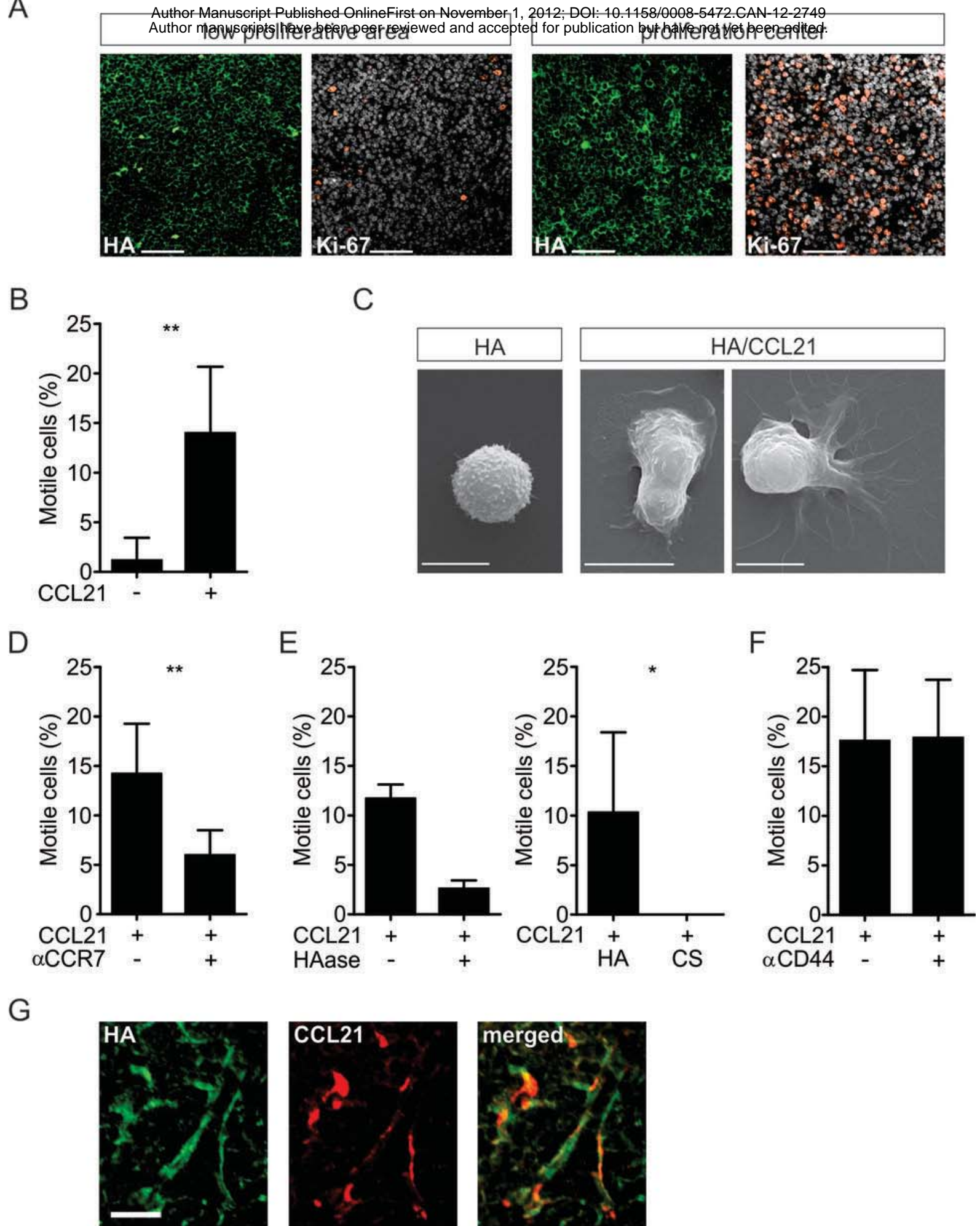


Figure 1. Girbl et al.

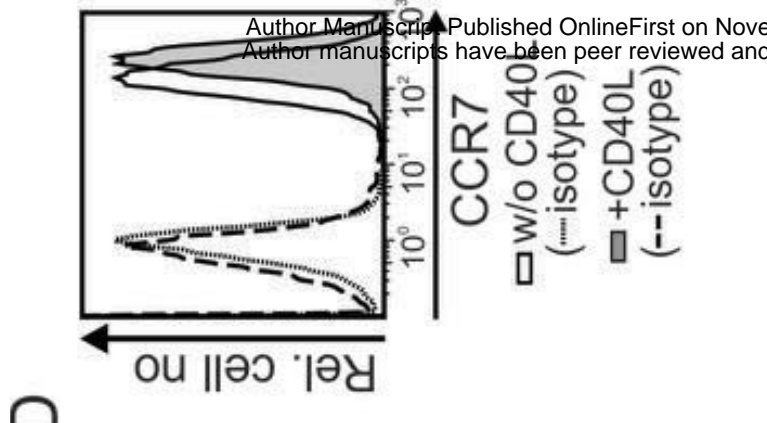
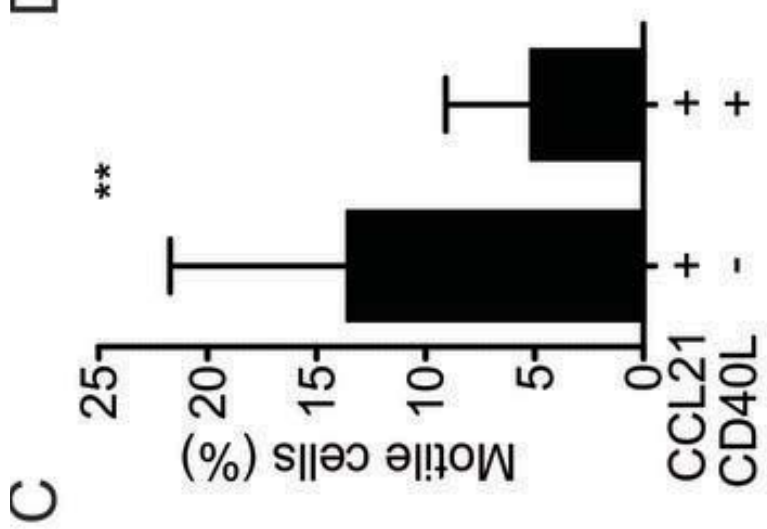
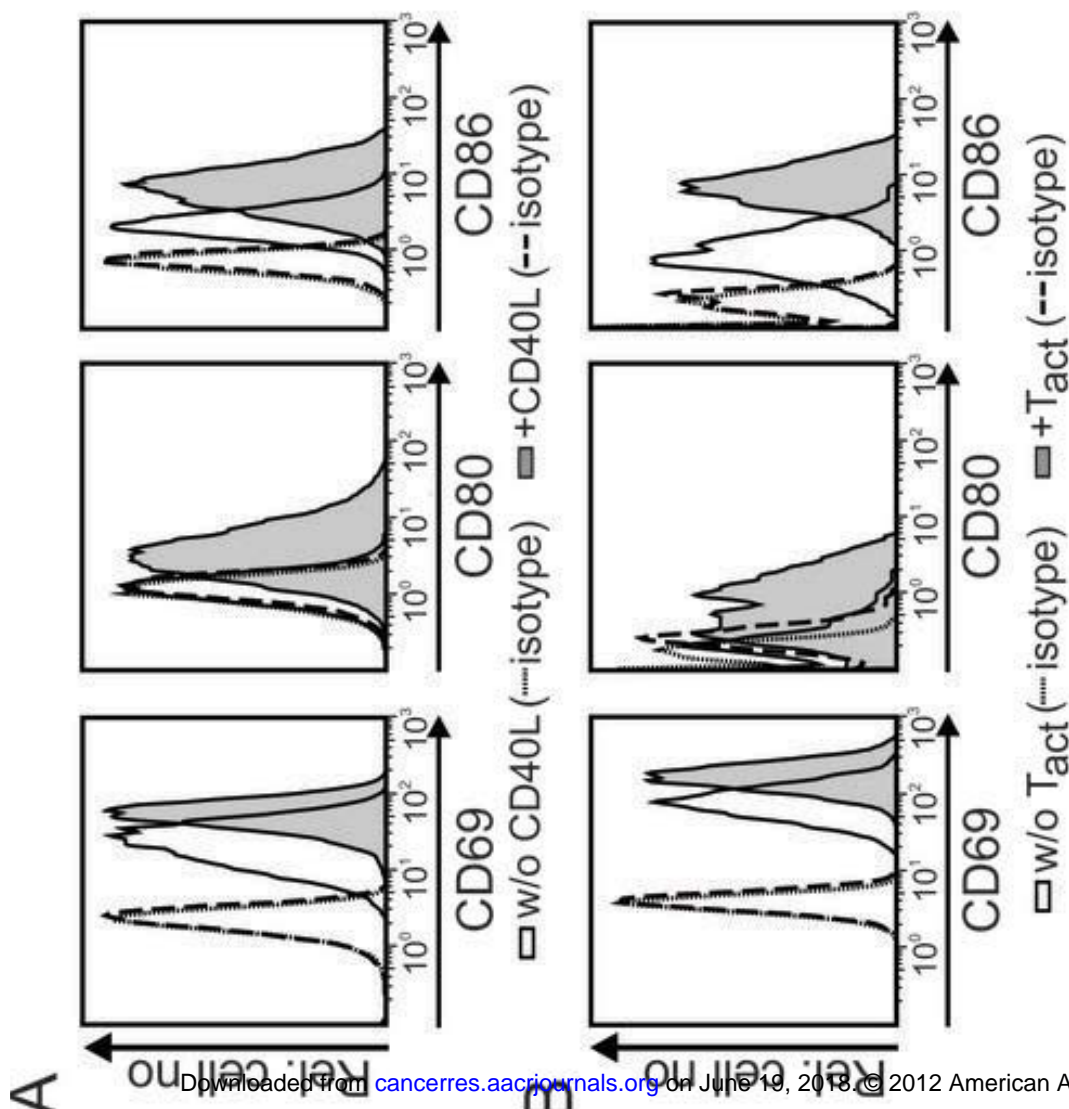


Figure 2. Girbl et al.

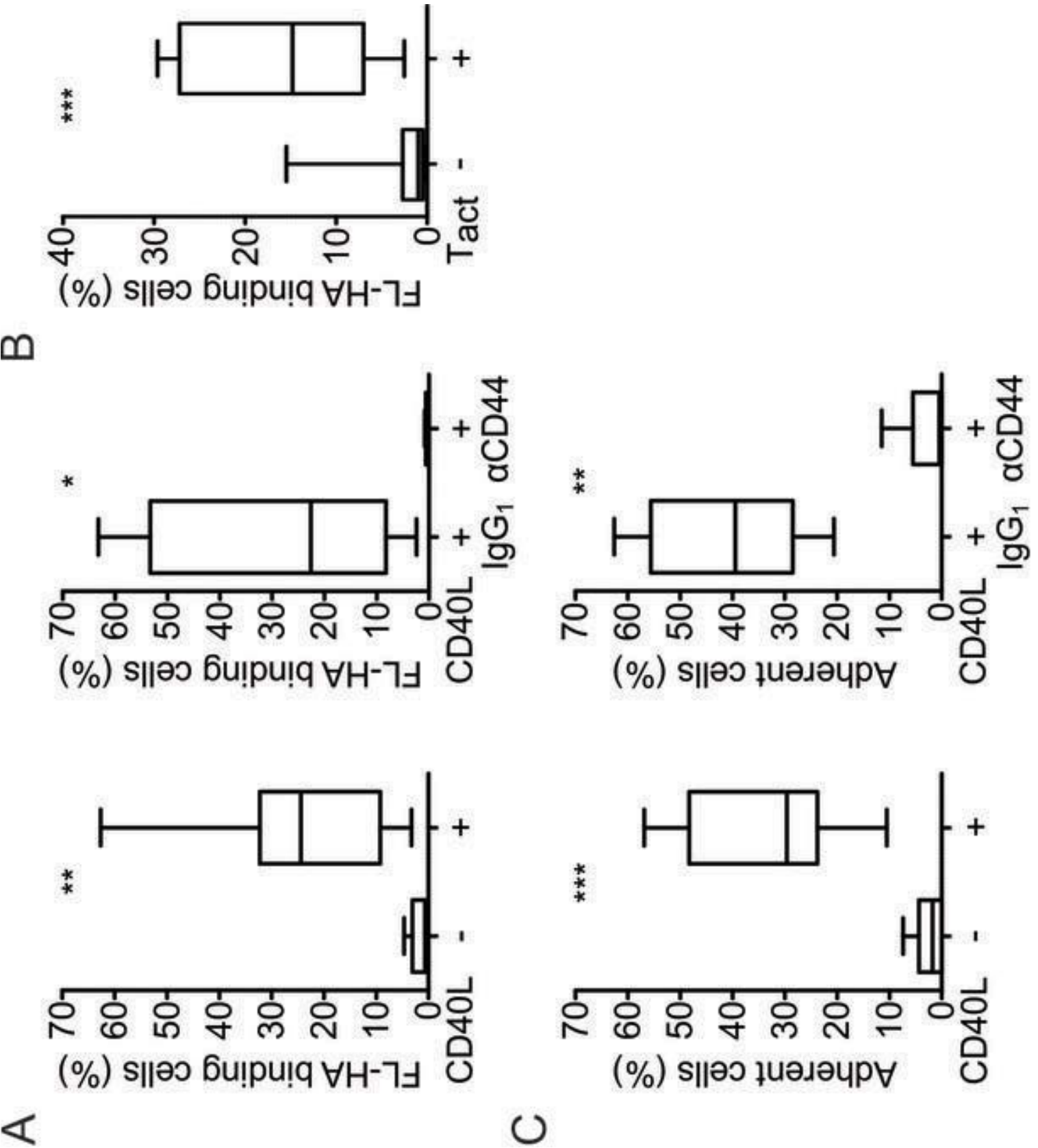


Figure 3. Girbl et al.

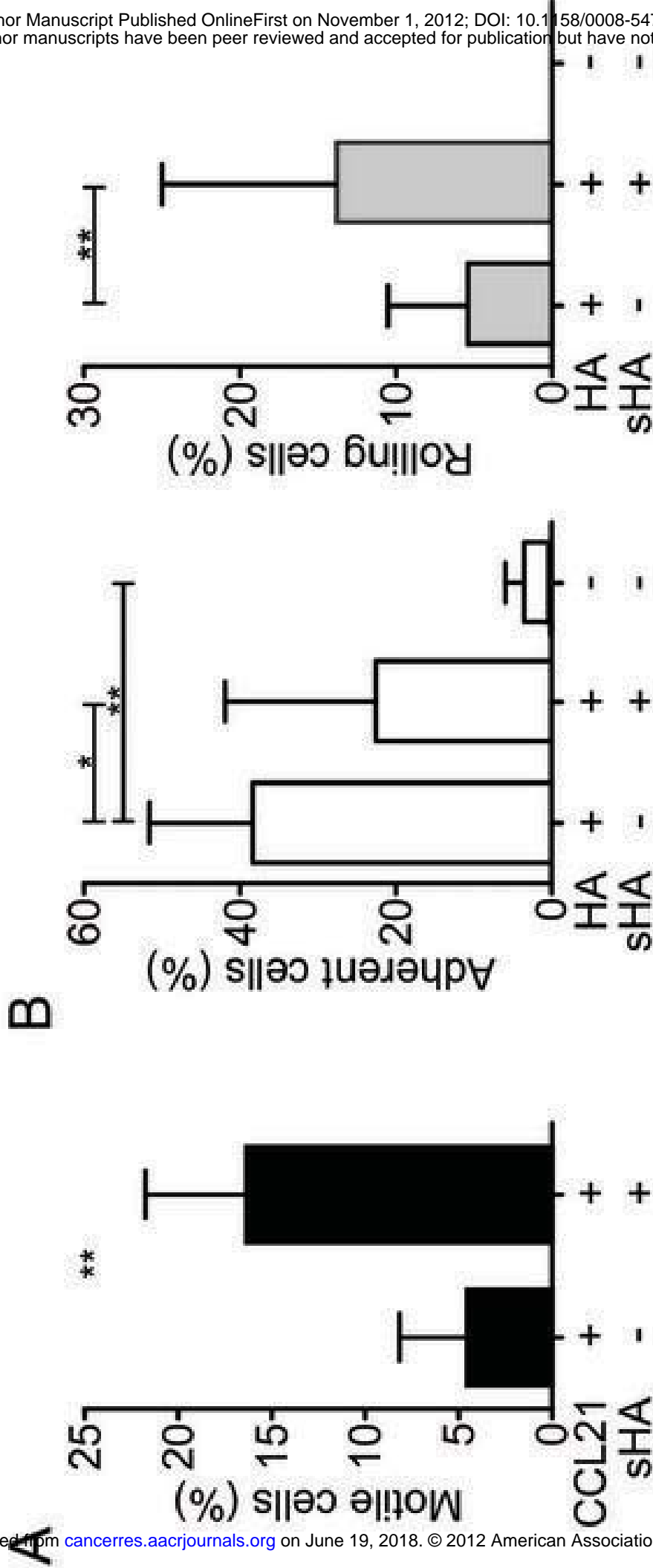


Figure 4. Girbl et al.

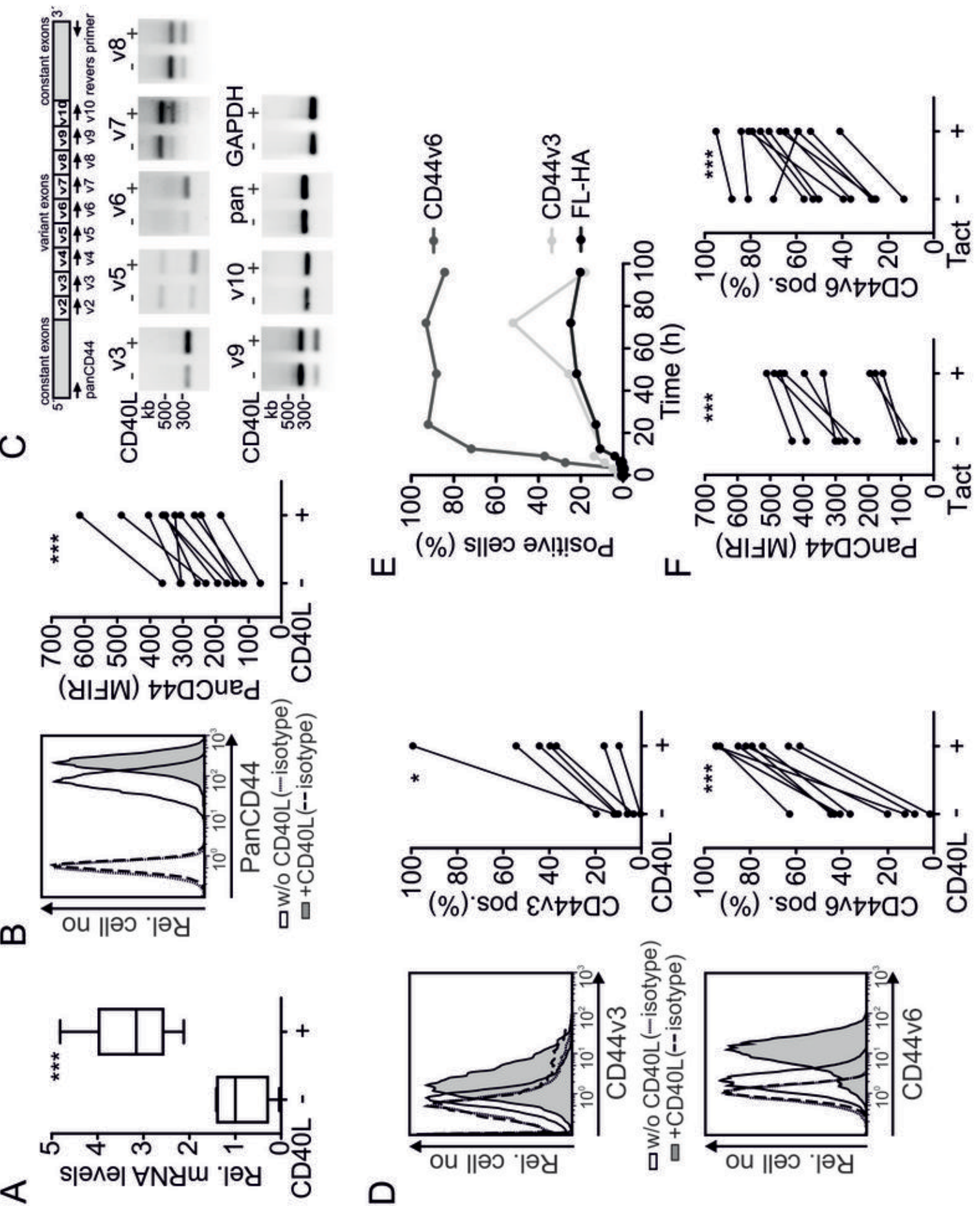


Figure 5. Giribl et al.

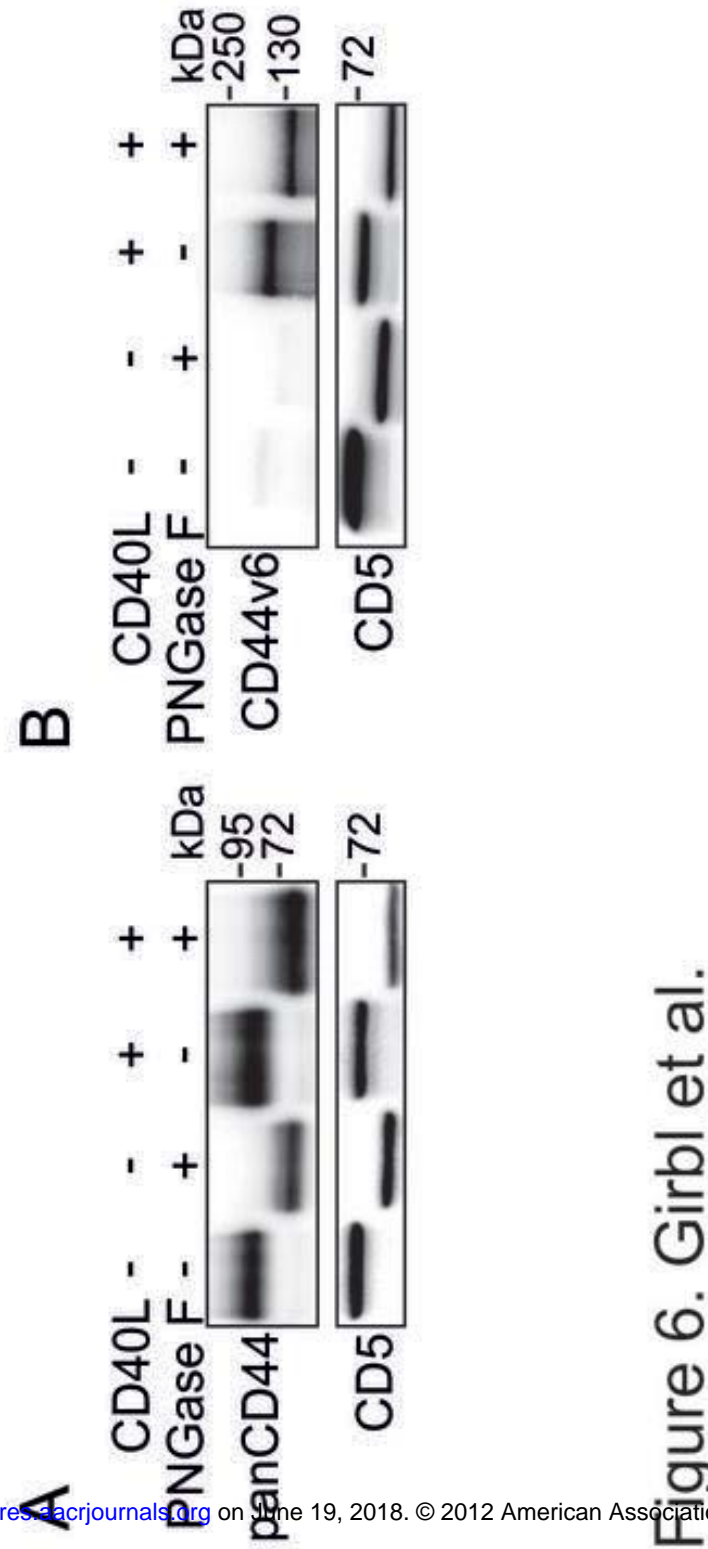


Figure 6. Girbl et al.

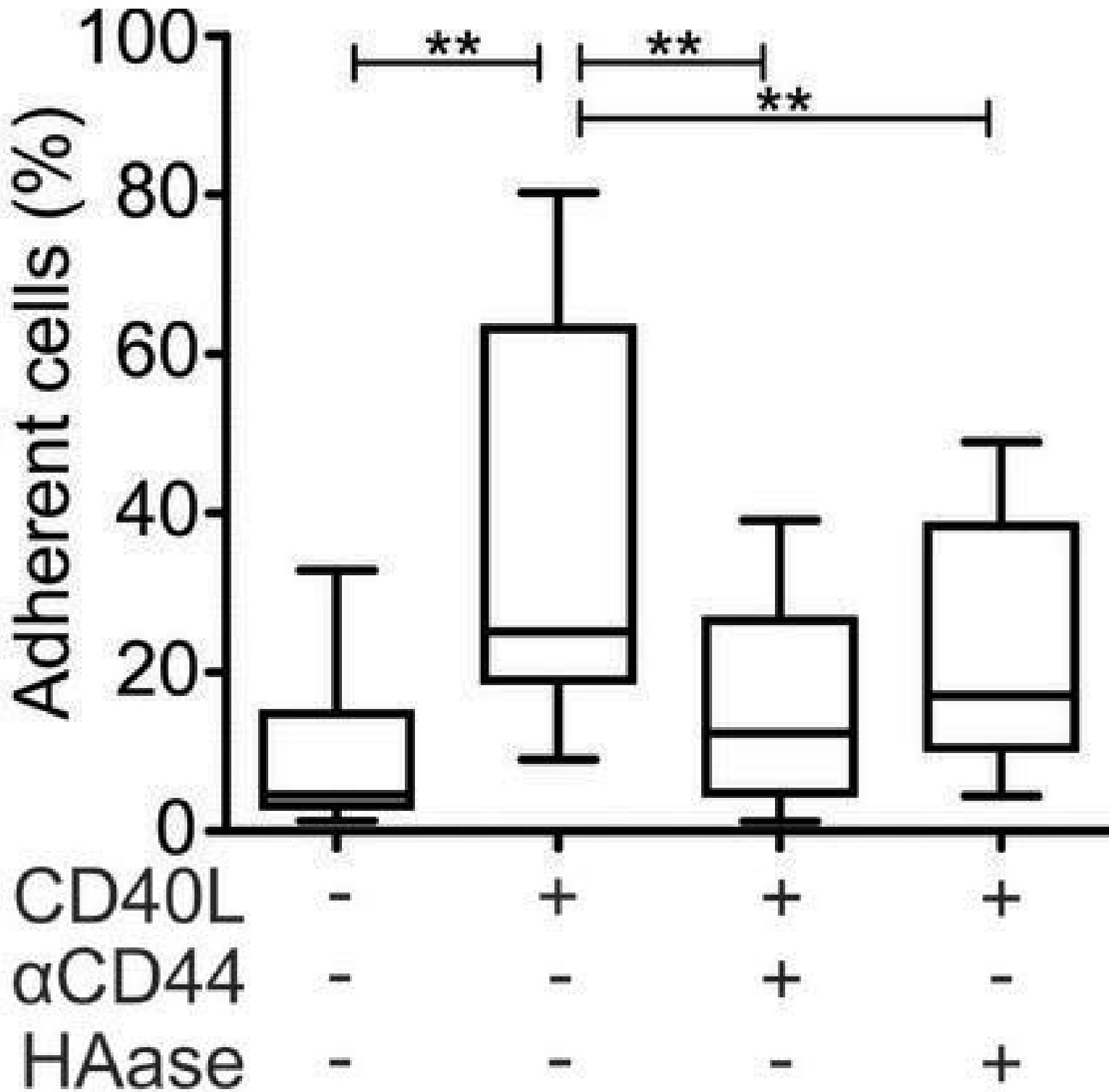


Figure 7. Girbl et al.

Cancer Research

The Journal of Cancer Research (1916–1930) | The American Journal of Cancer (1931–1940)

CD40-mediated activation of chronic lymphocytic leukemia cells promotes their CD44-dependent adhesion to hyaluronan and restricts CCL21 induced motility

Tamara Girbl, Elisabeth Hinterseer, Eva M Grössinger, et al.

Cancer Res Published OnlineFirst November 1, 2012.

Updated version	Access the most recent version of this article at: doi: 10.1158/0008-5472.CAN-12-2749
Supplementary Material	Access the most recent supplemental material at: http://cancerres.aacrjournals.org/content/suppl/2012/11/01/0008-5472.CAN-12-2749.DC1
Author Manuscript	Author manuscripts have been peer reviewed and accepted for publication but have not yet been edited.

E-mail alerts	Sign up to receive free email-alerts related to this article or journal.
Reprints and Subscriptions	To order reprints of this article or to subscribe to the journal, contact the AACR Publications Department at pubs@aacr.org .
Permissions	To request permission to re-use all or part of this article, use this link http://cancerres.aacrjournals.org/content/early/2012/11/08/0008-5472.CAN-12-2749 . Click on "Request Permissions" which will take you to the Copyright Clearance Center's (CCC) Rightslink site.